

Gas ^3He NMR Probe for Cryogenic Environments

X. Fan,^{1,2} S. E. Fayer,² and G. Gabrielse^{2,*}

¹*Department of Physics, Harvard University, Cambridge, Massachusetts 02138, USA*

²*Center for Fundamental Physics, Northwestern University, Evanston, Illinois 60208, USA*

(Dated: March 27, 2025)

Normal NMR probes cannot be used to make high frequency resolution measurements in a cryogenic environment because they lose their frequency resolution when the liquid sample in the probe freezes. A gaseous ^3He NMR probe, designed and constructed to work naturally in such cryogenic environments, is demonstrated at 4.2 K and 5.3 Tesla to have a frequency resolution better than 0.4 part per billion. As a demonstration of its usefulness, the cryogenic probe is used to shim a superconducting solenoid with a cryogenic interior so it produces a magnetic field with a high spatial homogeneity, and to measure the magnetic field stability.

I. INTRODUCTION

Small liquid samples (e.g. water or acetone) have a very narrow NMR resonance linewidth [1], so they are frequently used to characterize the magnetic field produced by a superconducting solenoid. Unfortunately, such probes cannot be used with solenoid systems that have only low temperature interior volumes because the liquid samples would freeze and lose their narrow linewidth. Heaters or dewars installed to prevent freezing are not ideal as they can perturb the magnetic field being characterized.

We are particularly interested in characterizing the magnetic field within the cryogenic volume used to measure the electron and positron magnetic moments [2, 3]. The moment of a single isolated particle is deduced from spin and cyclotron frequencies measured to extremely high accuracy, both of which are proportional to the magnetic field. A spatial homogeneity on the order of a part in 10^8 over a centimeter and a time stability on the order of a part in 10^{10} per hour are needed in the location into which a 4.2 K apparatus that includes a 0.1 K Penning trap is to be inserted [4]. The electron and positron moments, the most accurately measured properties of elementary particles, test the most precise predictions of the standard model of particle physics [5] and provide the most sensitive direct test of its fundamental charge conjugation, parity and time reversal (CPT) symmetry invariance with leptons.

The ^3He gas NMR probe demonstrated here (Fig. 1) works naturally at cryogenic temperatures. It is demonstrated at 4.2 K but should work at lower temperatures. ^3He is used because it has a substantial nuclear moment and it remains a gas at low temperatures. The major challenges are that many fewer spins are typically available to make an NMR signal in a gas compared to a liquid in the same volume, and ^3He is extremely expensive. The polarization fraction is much larger at low temperature, but that still does not compensate the lower number of spins. In order to greatly increase the number of spins

without increasing the sample pressure to a dangerously level, ^3He is kept in a closed system that has a large reservoir in addition to a small NMR bulb. ^3He moves from the room temperature reservoir to the small probe volume when the latter is cooled to 4.2 K with the pressure inside the bulb remaining approximately constant. The result is a signal from a 4.2 K gas sample that is comparable to that from a room temperature water sample. The crucial NMR relaxation times T_1 , T_2 , and T_2^* for ^3He at 4.2 K are deduced from free precession NMR signals and spin echoes.

We illustrate the usefulness of the gas ^3He NMR probe by shimming and characterizing a new superconducting solenoid system with a cold bore. The 5.3 T magnetic field is mostly produced by a persistent current in a large superconducting solenoid. The persistent currents injected into 11 superconducting shim coils are adjusted to narrow the frequency width of the NMR signal. The narrow NMR resonance is then used to precisely measure the stability of the magnetic field.

Note that in non-cryogenic contexts, ^3He NMR precession signals have been observed using room temperature gas cells and much smaller magnetic fields [6]. Key to such measurements was using lasers to attain nearly complete initial polarization [7], much larger than is produced for a NMR sample in thermal equilibrium. This could be added to cryogenic NMR probe but it would add considerable complexity and was not required for the demonstrated precision.

II. SPIN ALIGNMENT

The NMR signal is proportional to the size of the net magnetic moment, M , of N spins in thermal equilibrium at temperature, T , given by

$$M = N\mu \tanh \frac{\mu B}{k_B T} \approx N\mu \frac{\mu B}{k_B T}, \quad (1)$$

where μ is the magnetic moment for each spin and k_B is the Boltzmann constant. The hyperbolic tangent factor is the net fraction of the spins that are thermally aligned. The approximation to the right in Eq. (1) suffices in all cases considered here.

* gerald.gabrielse@northwestern.edu

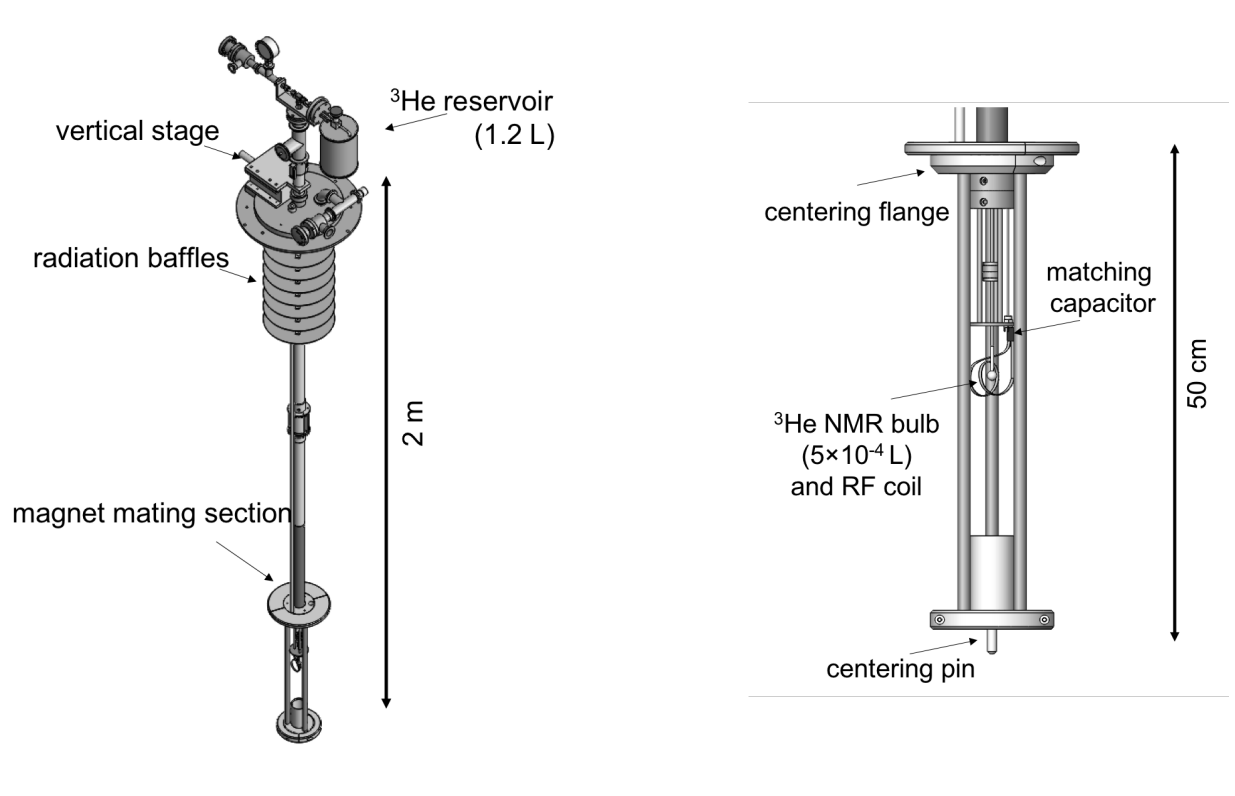


FIG. 1. (left) Overview of an NMR probe and a support designed to align with the axis of a superconducting solenoid being used for positron and electron measurements. The large room temperature reservoir is connected to the NMR bulb to ensure high density of ^3He target. The vertical translation stage makes it possible to raise and lower the NMR sample bulb. (right) Expanded view of the NMR sample bulb and its pickup coil. The centering flange and centering pin ensure that the bulb is radially aligned with the magnet. The RF coil is made of 99.9999 % purity copper and is loosely wound around the NMR bulb to minimize the residual magnetism. Matching capacitor is attached on a board near the bulb, see also Fig. 2. The magnetism of all components are carefully checked.

Since a room temperature water sample in a 1 cm diameter spherical cell produces a large and useful NMR signal, we compare the size of the water moment to that for ^3He gas in the same sample volume in Table I. The magnetic moments μ are given in nuclear magnetons μ_N . Since the ^3He moment is 76% that of water, most of the difference between the net moments comes from differing numbers of spins in the cell, N , and from differing polarization fractions, $\mu B/(k_B T)$.

| | μ/μ_N | N | $\mu B/(k_B T)$ | M/μ_N |
|---------------------------|-------------|----------------------|----------------------|----------------------|
| H_2O | 2.8 | 3.5×10^{22} | 1.8×10^{-5} | 1.8×10^{18} |
| ^3He (gas cell) | 2.1 | 1.3×10^{19} | 9.8×10^{-4} | 2.7×10^{16} |
| ^3He (reservoir) | 2.1 | 9.1×10^{20} | 9.8×10^{-4} | 1.9×10^{18} |

TABLE I. Comparison of NMR samples discussed at $B = 5.3$ Tesla. The values for H_2O are calculated at 300 K, and those for ^3He are calculated at 4.2 K. See text for details.

If we simply put an atmosphere of ^3He into the same sample cell and cooled it from 300 K to 4.2 K, the first ^3He line in the table shows that there would be ~ 2500 times fewer spins, a polarization factor increased by a factor of 54, and a net magnetic moment (and hence the

size of the NMR signal) only 1.6% that of a water sample.

Increasing the room temperature pressure inside a sealed bulb to match the water signal would require 60 atmospheres of pressure in the bulb at room temperature. Instead, we connect the 0.5 cm^3 glass bulb through a capillary to a much larger (1.2 liter) reservoir volume that stays at room temperature. Gas atoms move from the reservoir into the bulb to keep 1 atmosphere of pressure in the bulb as it cools to 4.2 K. The last line in the table shows that number of nuclear spins in the bulb is still 38 times smaller than for the water sample, but the polarization fraction is 54 times larger. The net result, when the slightly different nuclear moments are also factored in, is that the magnetic moment of the gas sample is 1.1 times that of the water sample. The NMR signal size is thus 10% bigger than the usable signal from room temperature water sample in the same volume.

Figure 1 shows the gas ^3He probe used in this demonstration. It was constructed to characterize a new superconducting solenoid system intended for electron and positron magnetic moment measurements. The 1 cm diameter glass bulb (Type I, Class A borosilicate glass, 529-A-12 Wilmad-LabGlass) was produced and measured to

have a low magnetism for NMR experiments. All the other components are carefully inspected to avoid residual magnetism. Special care was taken with the alignment parts in the magnet mating section, which were fabricated only from pure copper, aluminum, molybdenum and titanium. The RF coil near the bulb is made from a 99.9999 % pure thin copper foil, and is loosely wound around the bulb. The centering flange and centering pin ensure the radial alignment with our magnet. The ^3He line is mechanically fixed to the vertical stage at the hat, and can be moved inside the magnet bore. We can rotate NMR bulb, capillary line, and the electronics inside the magnet bore as one check of the residual magnetism of the probe.

III. NMR SPIN PRECESSION SIGNAL

The NMR probe is mainly operated at $B = 5.3$ T, which corresponds to a ^3He spin precession frequency of $\omega_0/2\pi = 172.3$ MHz. The homogeneity is optimized by changing the currents on 11 shim coils (specifically X, Y, ZX, ZY, XY, X^2-Y^2 , Z^2X , Z^2Y , Z^1 , Z^2 and Z^3). The circuit used to detect the NMR signal from the ^3He is a simple switching circuit shown in Fig. 2. Two RF frequency generators referencing a GPS clock signal are used. One drives the ^3He spin at the resonant frequency, and the other is used to mix down the NMR signal down to roughly 1.5 kHz. Then the signal is recorded by an Analog-to-Digital converter (ADC). Both frequencies are monitored by a spectrum analyzer. A pulse-controlled single pole, double throw (SPDT) RF switch is used to switch driving and detection side. Since the signal isolation of the SPDT switch is not enough, another RF switch is used in the driving side to suppress direct feedthrough. Three RF amplifiers are used to help driving and detecting the NMR target. A matching capacitor is mounted near the NMR RF coil in the liquid helium, to form a resonant circuit with a Q-factor of about 100, which increases both driving and detection efficiency.

In a thermal equilibrium at temperature T , the population in the lower of the two spin states is slightly less as described in Eq. 1. The ^3He bulb has the net magnetic moment given in the last line of Table I. A nearly resonant drive pulse tips the resulting magnetic moment vector by an angle $\pi/2$, as is typical in pulsed NMR measurements. The size of the NMR signal depends upon the length of the drive pulse and on the drive intensity, as well as on the net magnetic moment. Fig. 3 shows how the initial signal size varies as a function of the length of the drive pulse.

The polarization, now tipped perpendicular to the magnetic field direction, rotates at the angular NMR frequency ω_0 around the magnetic field direction. The changing flux through the pickup coils induces an electromagnetic field across the coil that is detected. Fig. 4 shows how the free induction decay (FID) signal at 5.3 T, mixed down to about 1.5 kHz, decays with a time con-

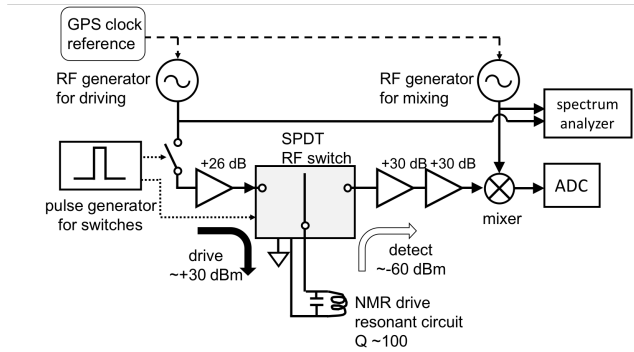


FIG. 2. The circuit used to drive and detect a $\omega_0/2\pi = 172.3$ MHz NMR signal. Two RF generators with GPS clock reference are used to drive and detect the NMR signal. Pulse-controlled RF switches are used to switch driving and detection. A resonant circuit with a Q-factor about 100 is prepared to increase the signal. See text for details.

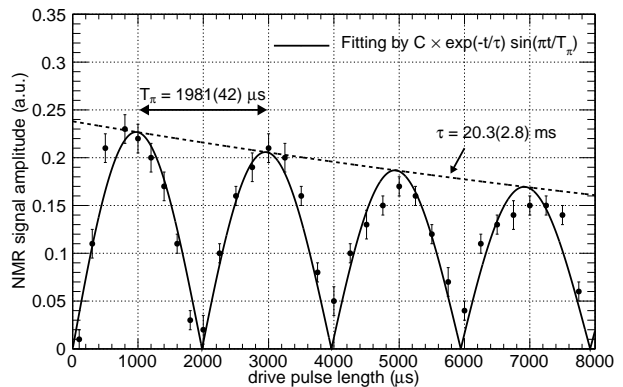


FIG. 3. The magnitude of the NMR precession signal depends upon the strength and length of the drive pulse, the latter being varied here. Each peak in the graph correspond to $\pi/2$, $3\pi/2$, $5\pi/2$, and so on, respectively. The decay constant is due to the inhomogeneity of the RF drive intensity. By taking this scan, we can measure the pi-pulse drive length T_π .

stant $T_2^* = 52\text{ms}$, as field inhomogeneity in the sample causes the precessing nuclear spins to get out of phase with each other. A Fourier transform of this oscillating signal shows a sharp peak at the spin precession frequency (Fig. 5), with a signal-to-noise ratio about 160. The width of this resonance line divided by the drive frequency, 173 MHz, gives the inhomogeneity in the NMR bulb, 24 ppb. The plot in the figure insert shows that the Fourier transform has wider “tails”. This is not surprising given that the ^3He gas in the glass capillary, just above the glass cell, contributes to the NMR signal and the magnetic field in the capillary is different than in the center of the solenoid field. We thus concentrate upon the width of the central feature, shown in black line in the insert.

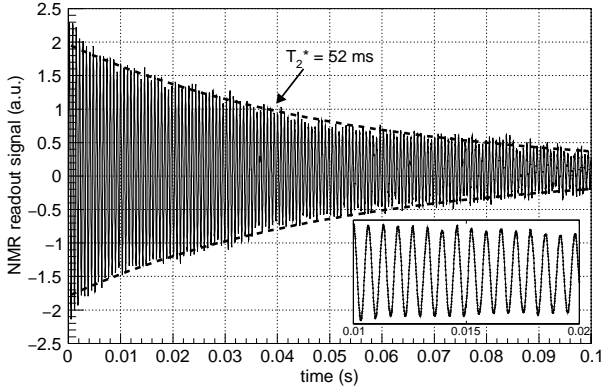


FIG. 4. The NMR spin precession signal from the ^3He nuclei at 5.3 T, mixed down from 172.3 MHz to 1.5 kHz, decays with a time constant $T_2^* = 52$ ms in this example. The dashed lines represent the exponential decay with T_2^* obtained by a fitting. The inset shows an expanded view of the same plot from 0.01 s to 0.02 s. A clear sinusoidal oscillation is observed.

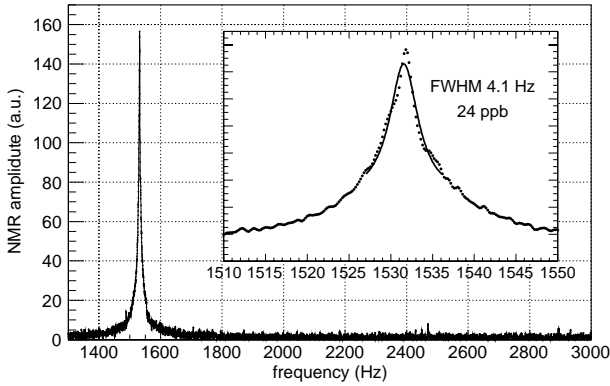


FIG. 5. Fourier transform of the NMR spin precession signal shown in Fig. 4. The signal-to-noise ratio is about 160. The inset shows an expanded view of the NMR peak. A Lorentzian fitting of this peak gives a FWHM of 4.1 Hz, which corresponds to 24 ppb relative inhomogeneity.

IV. VERTICAL AND HORIZONTAL RELAXATION TIME CONSTANTS

There are three time constants that are important in NMR measurements, T_1 , T_2 , and T_2^* . T_1 is the vertical relaxation time constant. T_2 is the decoherence time that would arise if the external magnetic field was perfectly homogeneous. It is the effect of the fluctuating magnetic field of the spins upon each other and limits the linewidth of a NMR probe. T_2^* is the NMR signal decoherence time that arises because of the magnetic field inhomogeneity in the magnetic field of the solenoid system. The best T_2^* we have achieved is $T_2^* = 52$ ms, as shown in Fig. 4. Here we discuss the measurement of T_1 and T_2 .

A. Measurement of vertical time constant T_1

The time constant T_1 characterizes the time required for the initial thermal imbalance between the two spin states to be reestablished. Some measurements report T_1 of ^3He as long as 1 day [8–11], and we were initially worried that this time constant was so long that it might be difficult to make measurements separated by only short times.

We measure T_1 of our ^3He sample by the saturation recovery method [12]. First a very long pulse drive compared to the T_π is applied several times to randomize the spins of the ^3He species. Then wait for a certain length of time for the total magnetization of ^3He to “recover.” After that, apply a $\pi/2$ pulse to measure the magnitude of the NMR signal after the recovery time. The time evolution of the magnetization $M(t)$ follows

$$M(t) = M_0 \left[1 - \exp\left(-\frac{t}{T_1}\right) \right], \quad (2)$$

where M_0 is the magnetization of the ^3He target after long enough time, calculated from Eq. 1.

The T_1 measurements with this method is shown in Fig. 6. We also varied some parameters of the setup as systematic checks. In Fig. 6, (i) default setup refers to the same setup in Figs. 3, 4, and 5. As for the other measurements, (ii) a 6 dB RF attenuator is put in after the 26dB amplifier on the drive side, (iii) the RF drive frequency is 2.5 kHz detuned from the resonant frequency, and (iv) z shim coil is intentionally ramped to make the homogeneity worse. All measurements are consistent within their error bars. By assigning the largest discrepancy between them as the systematic error and taking weighted mean of them, the vertical relaxation time is calculated to be $T_1 = 364$ (31) s. The time constant from magnetic dipole interaction is much longer than the measured value above [8, 10, 11, 13, 14], and thus in our system, the wall relaxation is dominant. Similar results of T_1 measurements have been reported [9, 15, 16].

Even this long T_1 time does not limit the application of our NMR probe. Due to the good signal-to-noise ratio achieved in our setup, as shown in Fig. 5, measurements with the recovery time of 20 seconds still give a signal-to-noise ratio of about 10. Usually we spend about this much time to change the current on shim coils to avoid quenching. Signal-to-noise ratio of 10 is good enough to see the effect of changing current on shim coils. When we monitor the drift of the superconductive magnet, we usually take the NMR signal every 60 seconds. The drift rate of the magnet is much slower than the vertical time constant T_1 , see also Sec. VI.

B. Measurement of horizontal time constant T_2

T_2 is the relaxation time constant of horizontal magnetization even when the external magnetic field is perfectly homogeneous. This limits the coherence time of

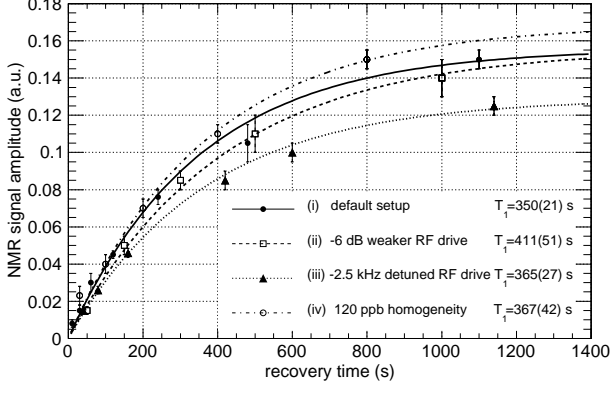


FIG. 6. Measurement of the vertical relaxation time T_1 with saturation recovery method. The dots are measured data and the lines are fittings by Eq. 2. Several parameters are varied to check the consistency. See texts for details.

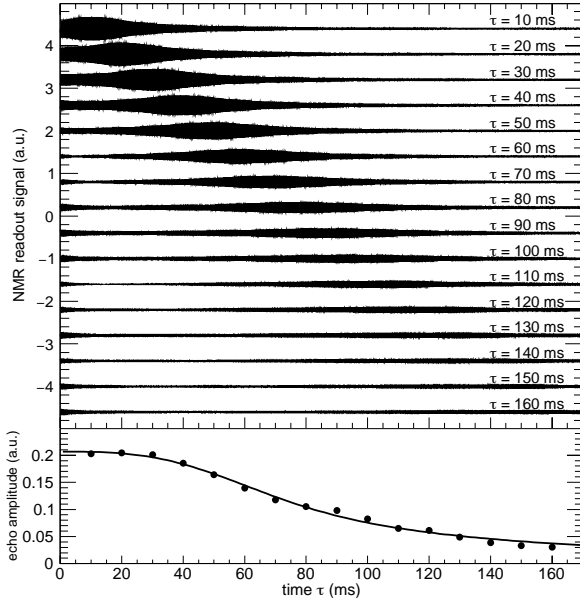


FIG. 7. (top) Spin echo signals observed with the ^3He NMR probe. Horizontal axis is the time after applying π pulse. Measurements with 16 different echo times τ are shown. (bottom) Amplitudes of the echo are plotted as a function of echo time τ . Solid line is a fitting by Eq.(3) without the T_2 term. See text for details.

the NMR decay and thus sensitivity on inhomogeneity of the magnetic field. Note that the ^3He species are moving at a speed as fast as $v_{\text{ave}} = \sqrt{8k_B T / \pi m} = 172$ m/s, and the relaxation timescale of ^3He is at the scale of second. Thus, the effect of diffusion is not negligible in the setup.

Figure 7 shows the spin echo measurements [17] performed with the probe. In the graphs, $\pi/2$ pulse and π pulses are applied at $t = -\tau$ and $t = 0$ respectively. In

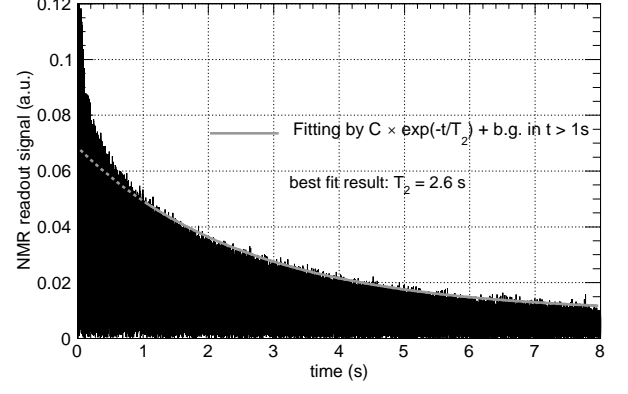


FIG. 8. CPMG spin echo decay of ^3He measured by the probe with the echo time $\tau = 5$ ms. The grey line shows an exponential fitting in $t > 1$ s, which gives $T_2 = 2.6$ s as the best fit result. The fast decay signal at the beginning is due to diffusion of the ^3He and quadratic magnetic field in our NMR volume [18, 19]. See text for details.

the top graph, the interval between the $\pi/2$ pulse and the π pulse, τ , is varied among 16 different values. Clear echos corresponding to each τ are observed. The bottom graph shows the amplitudes of the echos as a function of τ . As mentioned above, the ^3He species are moving quickly through the cell volume so the decay of the echo signals is dominated by the effect of diffusion. Since the data were taken after shimming the magnet, we assume the largest source of inhomogeneity is quadratic term of the magnetic field gradient. The amplitude of the first echo at $t = \tau$ as a function of the interval is given by [18, 19]

$$A(\tau) = \frac{\sqrt{\pi}}{2\beta\tau^{1.5}} \text{Erf}(\beta\tau^{1.5}) \exp\left(\frac{-2\tau}{T_2}\right) \quad (3)$$

$$\beta = \sqrt{\frac{8}{3} D \gamma^2 b^2 L^2}, \quad (4)$$

where b represents quadratic magnetic field gradient $B_z(\mathbf{r}) = B_0 + b z^2$, D is the diffusion coefficient, γ is the gyromagnetic ratio, L is half of the typical size of the target volume, and T_2 is the intrinsic horizontal decay constant. Fig. 8 shows the echo signal is fitted by Eq. 3 assuming $\beta\tau^2 \gg 2/T_2$. The best fit result gives $\beta = 0.0023 \text{ ms}^{-1.5}$.

The $\pm 2\sigma$ linewidth during these measurements is about 230 ppb. Based on the discussion of residual magnetism in Sec. V, we conservatively assume the uncertainty of this value to be ± 50 ppb. The typical straight line length of the bulb is $2L = \sqrt[3]{4\pi/3 \times (0.5\text{cm})^3} = 0.8$ cm. Thus we estimate $b = (7.6 \pm 1.7) \times 10^{-2} \text{ T/m}^2$. By using the gyromagnetic ratio of ^3He , $\gamma = 2\pi \times 32.434 \text{ MHz/T}$, the diffusion coefficient is calculated to be $D = (5.9 \pm 2.6) \times 10^{-7} \text{ m}^2/\text{s}$. This agrees with a previous measurement [20] at a lower magnetic field that found $D = 3.6 \times 10^{-7} \text{ m}^2/\text{s}$.

Based on the measurement above, we can set the interval time in Carr-Purcell-Meiboom-Gill (CPMG) pulse sequence and measure T_2 . The interval between CPMG pulses is set to be $\tau_0 = 5$ ms. With this echo time, the effect of diffusion is negligible as long as $T_2 \ll 1/\beta^2\tau_0^2 = 7500$ s. Figure 8 shows the CPMG spin echo signal. The initial rapid decay is a combined effect of diffusion and quadratic magnetic field [18, 19]. The exponential decay at longer time scale gives the time constant T_2 . An exponential fitting in $t > 1$ s gives a horizontal relaxation time constant $T_2 = 2.6$ s. Similar results have been obtained by a room temperature NMR measurement [21].

We also performed this measurement with different π pulse lengths. The π pulse length are varied by $\pm 3\%$, and the measured T_2 values fluctuates between 2.56 s and 2.81 s. We take this spread as a systematic error and estimate $T_2 = 2.7(2)$ s. The corresponding relative inhomogeneity is $1/(\omega_0 T_2) = 0.34(3)$ ppb. This is much smaller than the linewidth we have achieved and thus does not limit the performance of our probe.

V. POSSIBLE MAGNETISM OF THE PROBE

In the end, a measurement that requires a high field homogeneity will need to have the magnetic field shimmed to take out the unavoidable magnetism of the measurement apparatus. The magnetism of the NMR probe itself is one example. At the level of relative inhomogeneity we are interested in, $\mathcal{O}(10^{-9})$, the magnetism of the probe is not necessarily negligible. In order to estimate the residual magnetism of the NMR probe itself, our NMR probe is designed so that the NMR bulb and its support structure can be rotated inside the magnet bore from the top of the dewar. Figure 9 shows our superconducting solenoid system with the NMR probe inserted into the cold bore. The center rod that supports the NMR bulb is connected all the way to the top of the dewar. We can rotate the NMR bulb, capillary line and its supports, the electronics circuit board, and the RF coil. Note that the magnet mating parts in Fig. 1 do not rotate, but they are made of pure copper and aluminum, and far from the bulb, while the rotatable parts are made by variety of materials and some of them are quite close to the bulb. Thus the magnetism from the rotatable parts are estimated to be much higher than that from others.

After shimming the magnet, we rotate the probe to check the residual magnetism. Fig. 10 shows the result. The 0 degrees of the azimuthal angle is defined as the initial position of the probe, and the initial center frequency is defined as 0 in the left axis. Dependence on the azimuthal angle can be seen. At the worst angle, 225 degrees, the linewidth increases up to about 100 ppb, while the best linewidth is about 50 ppb. Thus the effect of the residual magnetism is estimated to be 50 ppb.

Possible candidates for the residual magnetism in the probe have been investigated. The magnetic field from a

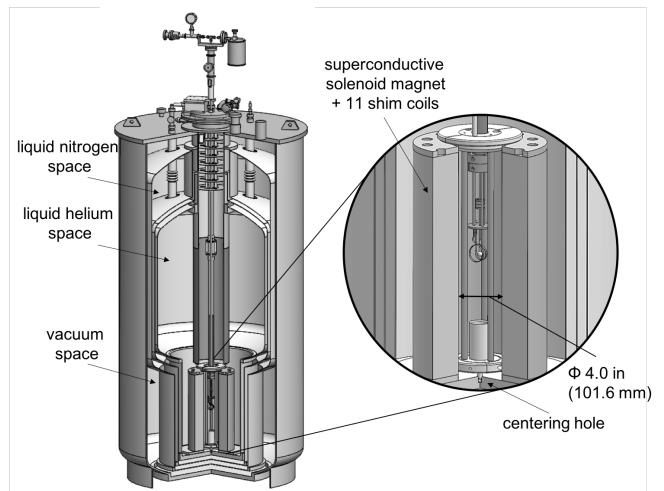


FIG. 9. The superconducting solenoid system with the ^3He NMR probe inserted into the 4.2 K cold bore. The bore size is 4.0 inches (101.6 mm) in diameter. It has 11 superconductive shim coils that can be used to optimize the homogeneity, in addition to the main 5.3 T solenoid magnet. The magnet is submerged in a liquid helium bath and thus the bore is always filled by liquid helium. NMR probe's centering plate and pin mate with the magnet structure as shown in the figure.

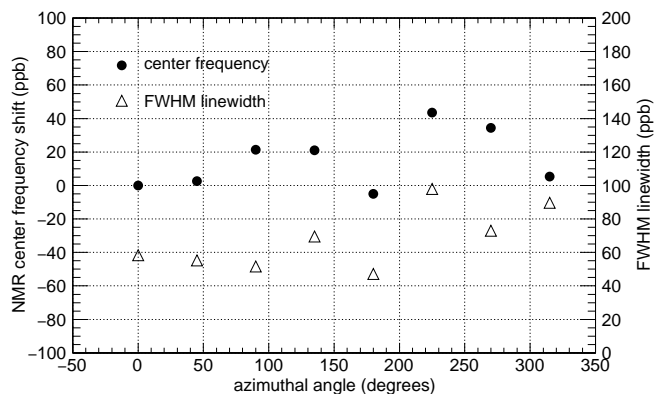


FIG. 10. Dependence of the NMR center frequency and linewidth on the azimuthal angle of the probe. The initial orientation of the probe is defined to be 0 degrees. Both the center frequency and the linewidth depend on the angle of the NMR probe. The residual magnetism of the NMR probe can be estimated by the change of the center frequency and linewidth. See text for details.

magnetized material with μ is given by

$$\mathbf{B}(r, \theta) = \frac{\mu_0 \mu}{4\pi r^3} (2 \cos \theta \hat{\mathbf{r}} + \sin \theta \hat{\boldsymbol{\theta}}), \quad (5)$$

where r is the distance from the material, θ is the polar angle with respect to the direction of μ , and μ_0 is the vacuum permeability. As can be seen, the effect from residual magnetism is proportional to r^3 . The closest part has by far the largest contribution to the magnetic field inhomogeneity.

In our case, the closest part is the RF copper coil. The magnetism of the 99.9999% purity copper foil that is used in the NMR probe is measured by a SQUID magnetometer (MPMS 3, Quantum Design Inc. [22]) to be $(5.0 \pm 1.2) \times 10^{-5}$ J/T cm³ at 5.3 T. Our coil is made of 0.1 mm×3 mm foil. Even with this small material, for example, if 1 cm of this foil is placed at 5 mm away from the NMR bulb, it will induce about 40 ppb inhomogeneity. This is as large as the rotational dependence we have observed. Searches for high Q-factor conductive metals with lower magnetism to replace the current copper coil are underway. Measurements using a small fragment of all other materials used (e.g. copper, tungsten, aluminum, circuit board, capacitor, SMA connector, glass of the bulb) suggest that these give smaller contributions.

VI. STABILITY OF A COLD BORE SOLENOID SYSTEM

The superconducting solenoid used for these studies (Fig. 9) was custom designed for positron and electron magnetic moment measurements carried out to test the most precise prediction of the standard model of particle physics [5]. For the lepton measurements, a Penning trap apparatus and a dilution refrigerator are lowered into the central bore of the superconducting solenoid system. For the measurements reported here, the NMR probe apparatus is inserted instead so that the bulb containing the ³He gas is at the location that a single lepton would be suspended.

The top of the metal form on which the solenoid is wound has a register that is used to center the NMR probe and the lepton trap apparatus, and a lower hole that allows a centering pin to center the inserted apparatus at the bottom of the solenoid. The lepton apparatus set directly upon the 4.2 K solenoid form so there can be no relative motion of the magnetic field and the apparatus making use of it.

The lepton measurements made so far requires the lepton spin and cyclotron frequencies using quantum jump spectroscopy. To achieve a smaller uncertainty the cyclotron frequency and the difference of the spin and cyclotron frequencies are actually measured. All of these frequencies are proportional to magnetic field, and this field dependence cancels out to lowest order since the magnetic moment depends on the ratio of these two frequencies. However, field variations are bad insofar as they increase the measured linewidths, and insofar as the two frequencies are measured at slightly different times, separated by about 1 min. To determine the electron magnetic moment to the current accuracy of 3 parts in 10^{13} , we have to perform spectroscopy at 3 parts in 10^{10} . For example, if we want to improve the limit by a factor of 10, the field needs be stable or corrected for drifts better than 1.8 ppb/h.

Once a narrow NMR linewidth is determined, we mea-

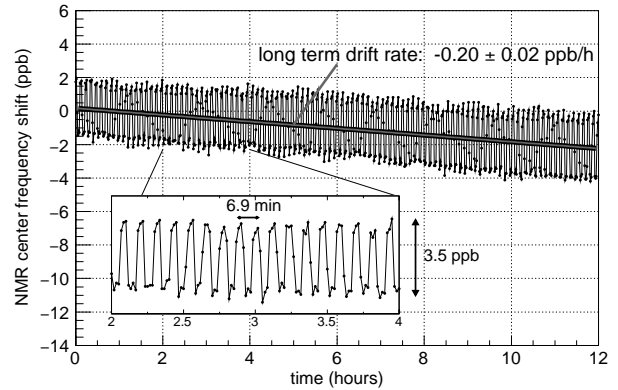


FIG. 11. Measurement of the ³He center frequency drift. ³He NMR signal is taken every 1 min and fitted by a Lorentzian to acquire center frequency. The long term drift rate is good enough to perform future magnetic moments measurement. The probe also reveals periodic oscillations that has never been observed. See text for details.

sure this frequency over and over to determine the field stability. We are interested in the stability on times over which we make individual frequency measurements, and the long term stability over the time that it takes to make the number of frequency measurements that must be averaged to get the desired uncertainty. The uncertainty in the NMR spin precession frequency in a single measurement is about 0.1 Hz, which corresponds to 0.5 ppb. By averaging the measurements over a long period, we can reduce the uncertainty on the drift rate.

Fig. 11 shows a set of measurements performed. The ³He NMR signal is taken every 1 min and is fitted by a Lorentzian to get the center frequency. The center frequency has been monitored for 12 hours, which show a drift less than 1.8 ppb/h, but it also revealed a surprising periodic and non-negligible oscillation. The average pressure in the helium space and the nitrogen space of the solenoid system are well regulated during this measurement. There are no obvious correlations with monitored temperatures, pressures, and flow rates in the helium and nitrogen dewars or ambient magnetic field, temperature, humidity, and atmospheric pressure in the lab. The drive and mixdown power and frequency were also monitored, but no obvious correlation was found. Studies, enabled by the gas NMR probe, are underway to understand and eliminate these oscillations.

VII. CONCLUSION

A gas ³He NMR probe at 4.2 K has a signal-to-noise and linewidth comparable to room temperature probe with the same volume that uses a liquid that is rich in hydrogen, such as water. A coupled reservoir-bulb system is key to attaining this signal-to-noise without requiring a dangerously high gas pressure. Several measurements

that are intrinsic to an NMR spectroscopy have been performed. We show that the gas probe is ideal for shimming and measuring the stability of superconducting solenoids with cryogenic bores.

VIII. ACKNOWLEDGEMENTS

J. Dorr, E. Novitski, and M. Dembecki contributed to an earlier version of this probe. This work was supported by the NSF, with X. Fan being partially supported by Masason Foundation.

-
- [1] R. Prigl, U. Haeberlen, K. Jungmann, G. zu Putlitz, and P. von Walter, Nuclear Instruments and Methods in Physics Research Section A: Accelerators, Spectrometers, Detectors and Associated Equipment **374**, 118 (1996).
 - [2] D. Hanneke, S. Fogwell Hoogerheide, and G. Gabrielse, Phys. Rev. A **83**, 073002 (2011).
 - [3] R. S. Van Dyck, Jr., P. B. Schwinberg, and H. G. Dehmelt, Phys. Rev. Lett. **59**, 26 (1987).
 - [4] S. F. H. Fogwell, J. C. Dorr, E. Novitski, and G. Gabrielse, RSI **86**, 053301 (2015).
 - [5] G. Gabrielse, S. E. Fayer, T. G. Meyers, and X. Fan, (in press. (2019).
 - [6] T. E. Chupp, M. E. Wagshul, K. P. Coulter, A. B. McDonald, and W. Happer, Phys. Rev. C **36**, 2244 (1987).
 - [7] T. R. Gentile, P. J. Nacher, B. Saam, and T. G. Walker, Rev. Mod. Phys. **89**, 045004 (2017).
 - [8] R. Chapman and M. G. Richards, Phys. Rev. Lett. **33**, 18 (1974).
 - [9] K. Luszczynski, R. E. Norberg, and J. E. Opfer, Phys. Rev. **128**, 186 (1962).
 - [10] N. R. Newbury, A. S. Barton, G. D. Cates, W. Happer, and H. Middleton, Phys. Rev. A **48**, 4411 (1993).
 - [11] C. P. Lusher, M. F. Secca, and M. G. Richards, Journal of Low Temperature Physics **72**, 25 (1988).
 - [12] J. B. Wooten, J. Jacobus, J. E. Gurst, W. Egan, W. G. Rhodes, and K. Wagener, Journal of Chemical Education **56**, 304 (1979).
 - [13] R. Chapman, Phys. Rev. A **12**, 2333 (1975).
 - [14] R. Barbé, F. Laloë, and J. Brossel, Phys. Rev. Lett. **34**, 1488 (1975).
 - [15] F. Kober, P.-. Wolf, J.-L. Leviel, G. Vermeulen, G. Duhamel, A. Delon, J. Derouard, M. Dcorps, and A. Ziegler, Magnetic Resonance in Medicine **41**, 1084 .
 - [16] W. Zheng, H. Gao, Q. Ye, and Y. Zhang, Phys. Rev. A **83**, 061401 (2011).
 - [17] E. L. Hahn, Phys. Rev. **80**, 580 (1950).
 - [18] P. Bendel, Journal of Magnetic Resonance (1969) **86**, 509 (1990).
 - [19] P. Le Doussal and P. N. Sen, Phys. Rev. B **46**, 3465 (1992).
 - [20] M. Himbert, J. Dupont-Roc, and C. Lhuillier, Phys. Rev. A **39**, 6170 (1989).
 - [21] F. Kober, B. Koenigsberg, V. Belle, M. Viallon, J. Leviel, A. Delon, A. Ziegler, and M. Dcorps, Journal of Magnetic Resonance **138**, 308 (1999).
 - [22] Quantum Design Inc., <https://www.qdusa.com/products/mpms3.html>.